

ELASTIC SCATTERING AND TOTAL CROSS SECTION AT THE CERN COLLIDER

UA4 Collaboration

(Amsterdam¹- CERN²- Genova³- Napoli⁴- Pisa⁵)

R. Battiston⁵, M. Bozzo³, P.L. Braccini⁵, F. Carbonara⁴, R. Carrara⁵,
R. Castaldi⁵, F. Cervelli⁵, G. Chiefari⁴, E. Drago⁴, M. Haguenaer²,
B. Koene¹, G. Matthiae⁴, L. Merola⁴, M. Napolitano⁴, V. Palladino²,
G. Sanguinetti⁵, G. Sciacca⁴, G. Sette³, R. van Swol¹, J. Timmermans¹,
C. Vannini², J. Velasco² and F. Visco⁴.

Presented by G. Matthiae

ABSTRACT

In the 1981 Collider run, proton-antiproton elastic scattering was measured in the range $0.05 < -t < 0.19 \text{ GeV}^2$. The t -distribution could be fitted by the exponential $\exp(bt)$ with slope parameter $b = 17.2 \pm 1.0 \text{ GeV}^{-2}$. Combining this data with the measurement of the inelastic interaction rate the total cross-section was found to be $\sigma_t = 66 \pm 7 \text{ mb}$. The ratio σ_{el} / σ_t is 0.20 ± 0.02 . In the 1982 run elastic scattering was measured in the range $0.21 < -t < 0.5 \text{ GeV}^2$. The t -distribution is well described by the slope parameter $b = 13.6 \pm 0.5 \text{ GeV}^{-2}$. A marked variation of the slope parameter with t takes place around $-t = 0.15 \text{ GeV}^2$ an effect similar to that previously observed at the ISR. Measurement of inelastic scattering are also discussed.

AIM OF THE EXPERIMENT

Experiment UA4 at the CERN Collider is devoted to the measurement of elastic scattering and of the total cross-section.

Elastic scattering events are observed by means of detectors placed inside movable sections of the SPS vacuum chamber ("Roman pots"). Each detector consists of a counter hodoscope and a wire chamber having resolution of 0.13 mm in the vertical and 0.4 mm in the horizontal coordinate¹⁾. The "Roman pots" are arranged in telescopes placed symmetrically with respect to the crossing point above and below the machine plane. Particles leaving the interaction region traverse the quadrupole of the machine and then reach these telescopes. Identification of elastic events is based on the requirement of collinearity.

The total cross-section is obtained by means of a method first used at the ISR²⁾. It is based on the simultaneous measurement of low- t elastic scattering and of the total inelastic rate. By using the optical theorem the total cross-section is obtained from the following expression

$$\sigma_t = \frac{16 \pi (\hbar c)^2}{1 + \rho^2} \frac{\left[\frac{dN_{el}}{dt} \right]_{t=0}}{N_{el} + N_{in}} \quad (1)$$

where ρ is the ratio of the real to the imaginary part of the forward elastic amplitude, while N_{el} and N_{in} are the observed rates of the elastic and inelastic interactions, respectively. The elastic differential rate at $t = 0$, $(dN_{el}/dt)_{t=0}$, is obtained by extrapolation. This method does not require an independent determination of the machine luminosity. In our experiment inelastic interactions are detected by telescopes of wire chambers and counter hodoscopes placed symmetrically on the left and right side of the crossing region, and covering the pseudorapidity range from 2.5 to 5.6.

Inelastic interactions of diffractive kind corresponding to the process $\bar{p}p \rightarrow \bar{p}X$ where the antiproton loses a very small fraction of its

initial momentum, are also observed in our system. Taking advantage of the deflection in the magnetic field of the machine quadrupoles, the momentum spectrum of the antiproton is measured.

RESULTS FROM THE FIRST COLLIDER RUN IN 1981

During the first physics run of the Collider elastic scattering at low- t and the total cross-section were measured at a centre-of-mass energy $\sqrt{s} = 540$ GeV. Data were taken in a short run (~ 15 hours) with luminosity of about 10^{26} cm $^{-2}$ s $^{-1}$ when the machine optics in the intersection region was the same as for normal SPS operation (normal- β optics). Elastic scattering was measured³⁾ in the four-momentum transfer range $0.05 < -t < 0.19$ GeV 2 . The collinearity plot in the vertical plane shows a peak with standard deviation $\delta\theta \approx 0.05$ mrad corresponding to a transverse momentum unbalance less than 15 MeV/c. Background of inelastic events was negligible. The observed t -distribution of about 1500 elastic events could be fitted by the exponential shape $\exp(bt)$ with slope parameter $b = 17.2 \pm 1.0$ GeV $^{-2}$.

Inelastic interactions were measured in the same run. It was ensured that the elastic and inelastic rates were obtained at the same luminosity by alternatively enabling the two triggers. The number of bunch crossing between the enabling and the occurrence of a trigger was recorded. The average rates of elastic and inelastic events were obtained from the total live times of the elastic and inelastic triggers respectively. The inelastic trigger was made as inclusive as possible by using a single-arm trigger in the pseudorapidity range $3.0 < \eta < 5.6$ in addition to a left-right trigger covering the same η -range in both hemispheres. The single-arm trigger allows detection of events that escape the left-right trigger, in particular single diffractive interactions. Beam-beam events are recognized by reconstructing a vertex from the observed tracks. The fraction of events escaping detection due to the limited coverage in polar angle of the detectors was estimated by extrapolation to be less than 2%.

The total number of elastic events was calculated from the observed number of events under the assumption of an exponential t -distribution with constant slope parameter $b = 17.2 \text{ GeV}^{-2}$ equal to the value measured in the accessed t -range. In that case, assuming $\rho = 0$, eq. (1) can be rewritten as

$$\sigma_t = 16 \pi (\hbar c)^2 \frac{b}{1 + \frac{N_{in}}{N_{el}}} \quad (2)$$

The ratio N_{in} / N_{el} was found to be 4.07 ± 0.22 . The measured value of the total cross section⁴⁾ is $\sigma_t = 66 \pm 7 \text{ mb}$. The quoted error is purely statistical and is mainly due to the uncertainty on the slope parameter. A graphical representation of this result, following from eq. (2) is shown in Fig. 1 where the data point corresponding to the maximum ISR energy is also shown for comparison. Our result on σ_t is plotted in Fig. 2 together with pp and $\bar{p}p$ data at lower energies. The full line in Fig. 2 is the result of the dispersion relation fit of ref. 5) which follows a $(\log s)^2$ dependence.

We also find $\sigma_{el} / \sigma_t = 0.20 \pm 0.02$ and $\sigma_{\text{"diff"}} / \sigma_t = 0.17 \pm 0.03$, where $\sigma_{\text{"diff"}}$ refers to the events having tracks in one hemisphere only. These values, within errors, are consistent with those observed in the ISR energy range.

The relevance of the Collider data for the understanding of the very high-energy behaviour of the elastic amplitude has been discussed by A. Martin⁶⁾. Our result on the slope parameter at low- t is compatible with the prediction of the Reggeon Field Theory⁷⁾. According to this theory, however, the raise of the total cross-section with energy is not as fast as suggested by our measurement. The prediction at the Collider is of about 55 mb.

The geometrical picture⁸⁾ of high-energy scattering which uses for the proton opaqueness a shape derived from the electro-magnetic form factor, predicts a too low value for the forward slope.

For a total cross-section of 66 mb, the prediction⁸⁾ is $b = 14 \text{ GeV}^{-2}$, which does not seem to be consistent with our experimental result.

Recently, fits of the available data on the slope parameter b over the FNAL and ISR energy range have been presented⁹⁾. Extrapolation of these fits to the Collider energy does not lead, however, to unambiguous conclusions.

PRELIMINARY RESULTS FROM THE 1982 RUN

Before the 1982 run our elastic scattering apparatus was implemented as shown in Fig. 3. The system, symmetric with respect to the crossing point, consists of sixteen detectors, each one placed in a "Roman pot", which are arranged in eight telescopes. The "inner" telescopes are at a distance of about 23 m from the crossing point, while the "outer" telescopes are at about 40 m. The minimum distance of the pots from the beam at which the detectors could still operate safely was found to be roughly equal to twenty times the r.m.s. value of the beam size, almost independently of the machine optics. This distance determines the minimum value of the scattering angle which depends on the optics in the intersection region. The range of t which is accessible for each optics and the Roman pot telescopes used in the measurement are listed in Table 1.

Table 1

Machine optics	$\beta_H \times \beta_V$ (m)	Roman pot telescopes	accessible t -range (GeV^2)
Normal - β	50 x 50	outer	0.05 - 0.19
High - β	100 x 100	outer	0.02 - 0.35
Medium - β	7 x 3.5	inner	0.2 - 0.5
Low - β	2 x 1	$\left\{ \begin{array}{l} \bar{p} : \text{inner and outer} \\ p : \text{inner} \end{array} \right.$	0.4 - 1.5

As seen from Table 1, our elastic scattering apparatus is quite flexible and allows to cover a rather wide range of t with some overlap between measurements done with different optics.

The angular resolution is determined by both the spatial accuracy of the detectors and the intrinsic angular spread of the beams which varies as $1/\sqrt{\beta}$. For the high- β optics the two effects are comparable in size giving rise to a collinearity distribution with r.m.s. value $\delta\theta \simeq 0.04$ mrad, while for the low- β optics the beam divergence dominates completely and the collinearity peak is much wider ($\delta\theta \simeq 0.2$ mrad).

The elastic trigger was provided by the coincidence of the trigger counters of the left and right arm. Usually, with stable beam conditions the fraction of good elastic events in the trigger was of 30 - 50%.

In the first few days of the 1982 run the Collider was operated with medium- β optics. Elastic scattering was measured using the "inner" telescopes in the range $0.21 < -t < 0.5$ GeV². The t -distribution of about 7.000 events is shown in Fig. 4. These data can be well fitted by an exponential shape. As a preliminary value of the slope we quote $b = 13.6 \pm 0.5$ GeV⁻².

In a short test run with high- β optics at low luminosity ($\sim 2 \cdot 10^{25}$ cm⁻²s⁻¹), about 700 elastic events were collected in the range $0.025 < -t < 0.19$ GeV². The observed t -distribution agrees with that measured in the 1981 run³⁾.

In Fig. 5 the data already published by UA1¹⁰⁾ and UA4³⁾ on the slope parameter b as a function of t are plotted together with our new preliminary result. Additional data from the UA1 Collaboration¹¹⁾ reported at this Conference are consistent with those shown in Fig. 5. It is clear that a fast variation of the slope is taking place at $-t \sim 0.15$ GeV², an effect which was first observed at the ISR¹²⁾. In Fig. 6 a compilation of the proton-proton results on the slope b as a function of t at $\sqrt{s} = 53$ GeV is presented. For each data point in Fig. 5 and 6 the horizontal bar indicates the range in t where the exponential fit was performed.

At $\sqrt{s} = 53$ GeV, when moving from $-t = 0.4$ GeV² down to $-t \lesssim 0.1$ GeV², the slope increases by $\Delta b \approx 2.5$ GeV⁻². While the shrinkage of the elastic peak from the ISR to Collider energy is well demonstrated by present data, it is not clear, however, whether the increase of the slope with energy is larger at very low values of t .

General arguments⁶⁾ indicate that if $\sigma_t \sim (\log s)^2$ and $\sigma_{el}/\sigma_t \rightarrow$ constant $\neq 0$, as $s \rightarrow \infty$, then $b(s, t = 0) \sim (\log s)^2$ but $b(s, t < 0) \lesssim \log s$.

The present experimental situation can be summarized as follows. For pp scattering at $\sqrt{s} = 53$ GeV, by taking the averages of available data we get:

$$\begin{array}{lll} \text{for} & -t \lesssim 0.1 \text{ GeV}^2 & b = 13.0 \pm 0.2 \text{ GeV}^{-2} \\ \text{for} & -t = 0.4 \text{ GeV}^2 & b = 10.4 \pm 0.2 \text{ GeV}^{-2} \end{array}$$

Then, using the UA4 results of Fig. 5, the change of slope from $\sqrt{s} = 53$ GeV to $\sqrt{s} = 540$ GeV is:

$$\begin{array}{lll} \text{for} & -t \lesssim 0.1 \text{ GeV}^2 & \Delta b = 4.2 \pm 1 \text{ GeV}^{-2} \\ \text{for} & -t = 0.4 \text{ GeV}^2 & \Delta b = 3.2 \pm 0.5 \text{ GeV}^{-2} \end{array}$$

More accurate data at very low t are needed in order to reach a conclusion.

The good spatial resolution of our wire chambers in the Roman pots allows to measure the antiproton momentum by tracking the trajectory through the Q_F and Q_D quadrupoles (see Fig. 3). For low- β optics, the bending of the first quadrupole pair Q_F in the vertical plane is roughly twice the scattering angle while the bending of the second pair Q_D is about equal to the scattering angle. The typical value of the scattering angle in the low- β optics is around 2.5 mrad. The \bar{p} momentum is determined by a best fit on the particle trajectory using the quadrupole transfer matrices with constraint on the vertical position of the interaction point. The momentum resolution, as determined experimentally on elastic events has standard deviation of $0.7 \cdot 10^{-2}$ as shown in Fig. 7. The main contribution to the observed resolution is from measurement errors. In fact the momentum spread of the beam is less than 10^{-3} and for the SPS quadrupoles the relative

variation of the integrated gradient across the aperture is less than $3 \cdot 10^{-3}$.

The measurement of the momentum is relevant for the rejection of inelastic background, especially in the low- β optics. In addition it allows to determine the momentum spectrum of the \bar{p} in the inelastic scattering reaction $\bar{p}p \rightarrow \bar{p}X$. Data have been taken using a trigger that demanded the four-fold coincidence of the four pots ("inner" and "outer") on the \bar{p} side together with at least a charged particle in the opposite hemisphere in the pseudorapidity range $3 < \eta < 5.6$. This trigger permits the study of the diffractive dissociation process with excitation of systems having large mass. An example of the momentum spectrum of the \bar{p} for the diffractive trigger is shown in Fig. 7.

REFERENCES

- 1) J. Buskens et al., Nucl. Instr. and Methods (1983), in print.
- 2) CERN-Pisa-Roma-Stony Brook Collaboration, Phys. Lett. 62B (1976) 460 and Nucl. Phys. B145 (1978) 367.
- 3) R. Battiston et al., Phys. Lett. 115B (1982) 333.
- 4) R. Battiston et al., Phys. Lett. 117B (1982) 126.
- 5) U. Amaldi et al., Phys. Lett. 66B (1977) 390.
- 6) A. Martin, Proceedings of the XXI International Conference on High Energy Physics, Paris 1982, p. 579, and Proceedings of this Conference.
- 7) J. Baumel et al., Nucl. Phys. B198 (1982) 13.
A.R. White, Proceedings of the XIII International Symposium on Multiparticle Dynamics, Volendam, 1982.
- 8) T.T. Chou and C.N. Yang, Phys. Rev. D19 (1979) 3268.
- 9) J.P. Burq et al., Phys. Lett. 109B (1982) 124;
M. Block and R. Cahn, CERN preprint TH 3342 (1982);
T. Ekelöf, Proceedings of the XVII Rencontre de Moriond on Elementary Hadronic Processes and Spectroscopy, les Arcs, 1982.
- 10) G. Arnison et al., Phys. Lett. 121B (1983) 77.
- 11) F. Ceradini, Contribution to this Conference.
- 12) G. Barbiellini et al., Phys. Lett. 39B (1972) 663.
- 13) U. Amaldi et al., Phys. Lett. 36B (1971) 504;
H. De Kerret et al., Phys. Lett. 68B (1977) 374;
L. Baksay et al., Nucl. Phys. B141 (1978) 1.
M. Ambrosio et al., Phys. Lett. 115B (1982) 495;
A. Breakstone et al., preprint IFUB 82/17.
N. Amos et al., Phys. Lett. 120B (1983) 460.

Figure Captions

- Fig. 1 Graphical presentation of our total cross-section measurement⁴⁾. The result at the maximum ISR energy is also shown for comparison.
- Fig. 2 Total cross-section for proton-proton and proton-antiproton interactions. The lines represent the dispersion relation fit of ref. 5).
- Fig. 3 Sketch of the elastic scattering layout showing the telescopes of Roman pots. The system is symmetric with respect to the crossing point. The small box inside each pot represents a detector consisting of a wire chamber and a counter hodoscope^{1,3)}. Q_F represents a pair of quadrupoles focusing in the vertical plane while Q_D is a defocusing pair. The \bar{p} trajectory in the vertical plane for 2.5 mrad scattering angle and low- β optics is also shown.
- Fig. 4 Preliminary t -distribution of about 7000 elastic scattering events. The result for the slope is $b = 13.6 \pm 0.5 \text{ GeV}^{-2}$.
- Fig. 5 The Collider data on the slope parameter b are plotted versus t . The published results from UA1¹⁰⁾ and UA4³⁾ are shown together with the new UA4 preliminary value. The horizontal bar indicates the range of t used in the exponential fit.
- Fig. 6 The ISR data^{12,13)} on the slope b for proton-proton scattering are plotted versus t . As in Fig. 5, the horizontal bar indicates the t -range of each measurement.
- Fig. 7 Momentum distribution of the antiproton for elastic scattering and inelastic diffractive events. The variable x is defined as the ratio of the measured momentum to the nominal beam momentum. These data are not normalized and not corrected for acceptance.

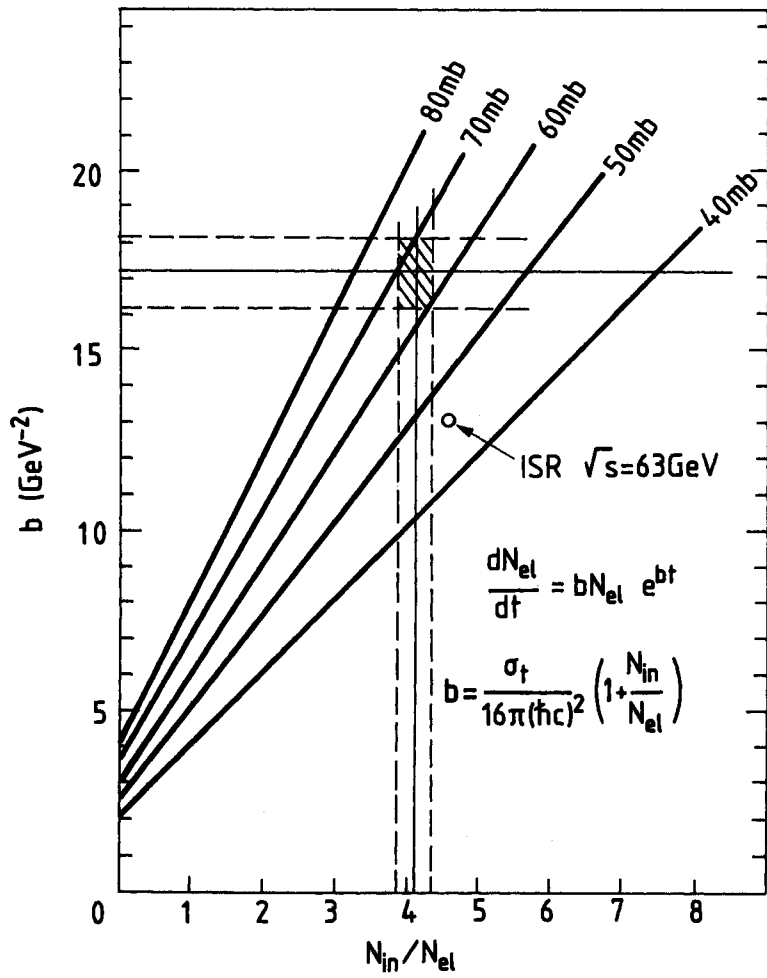


Fig. 1

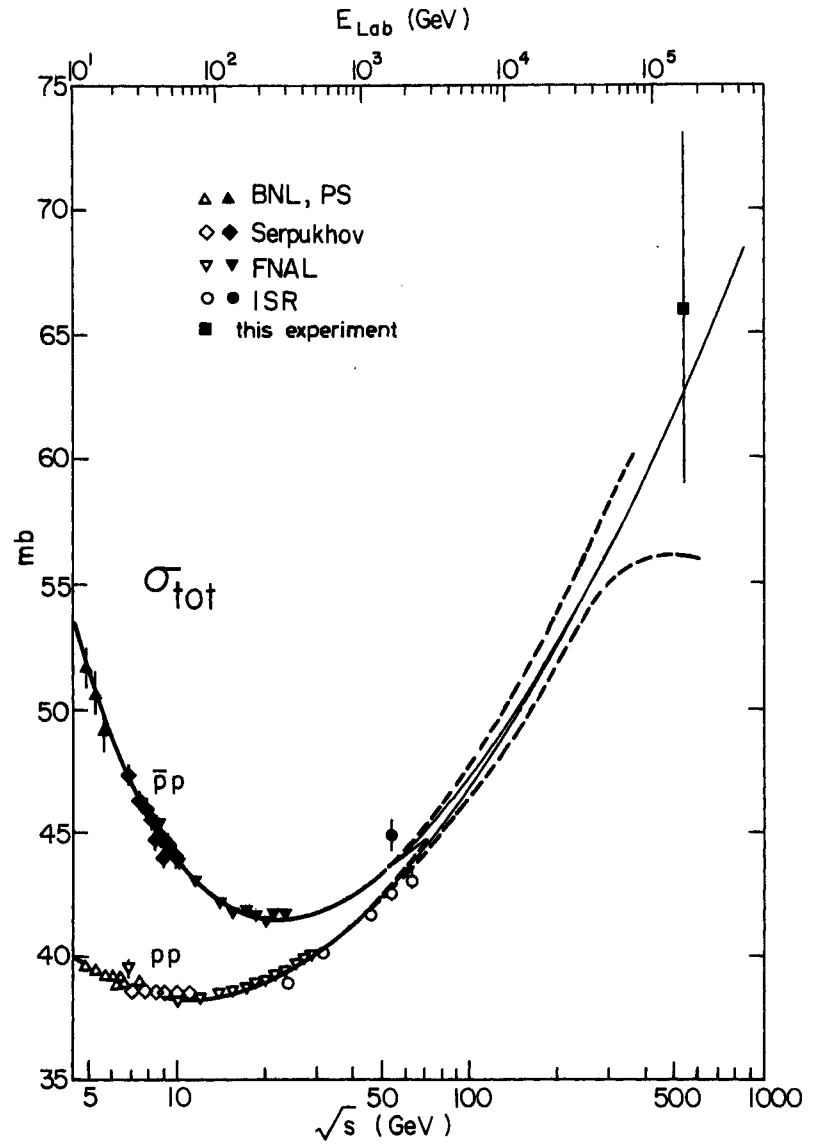


Fig. 2

ELASTIC SCATTERING LAYOUT

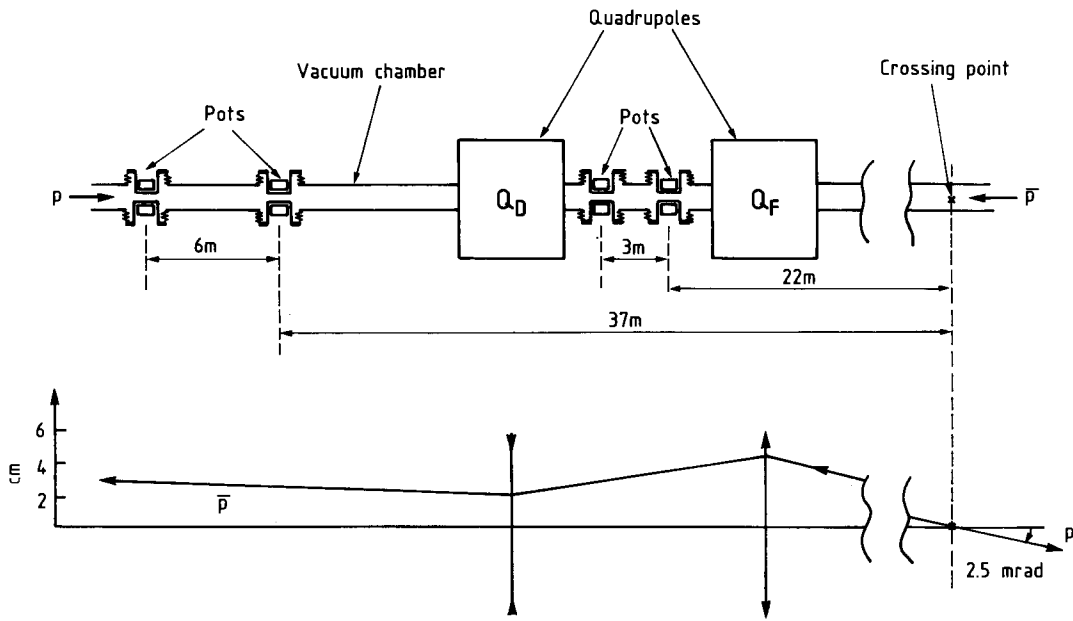


Fig. 3

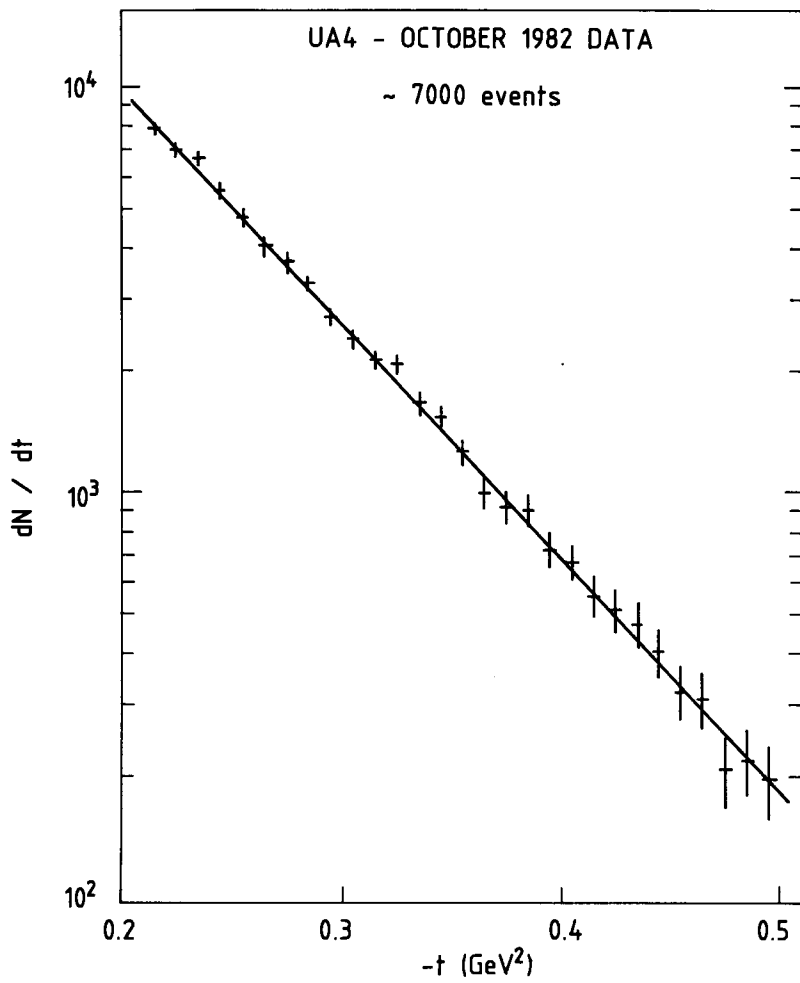


Fig. 4

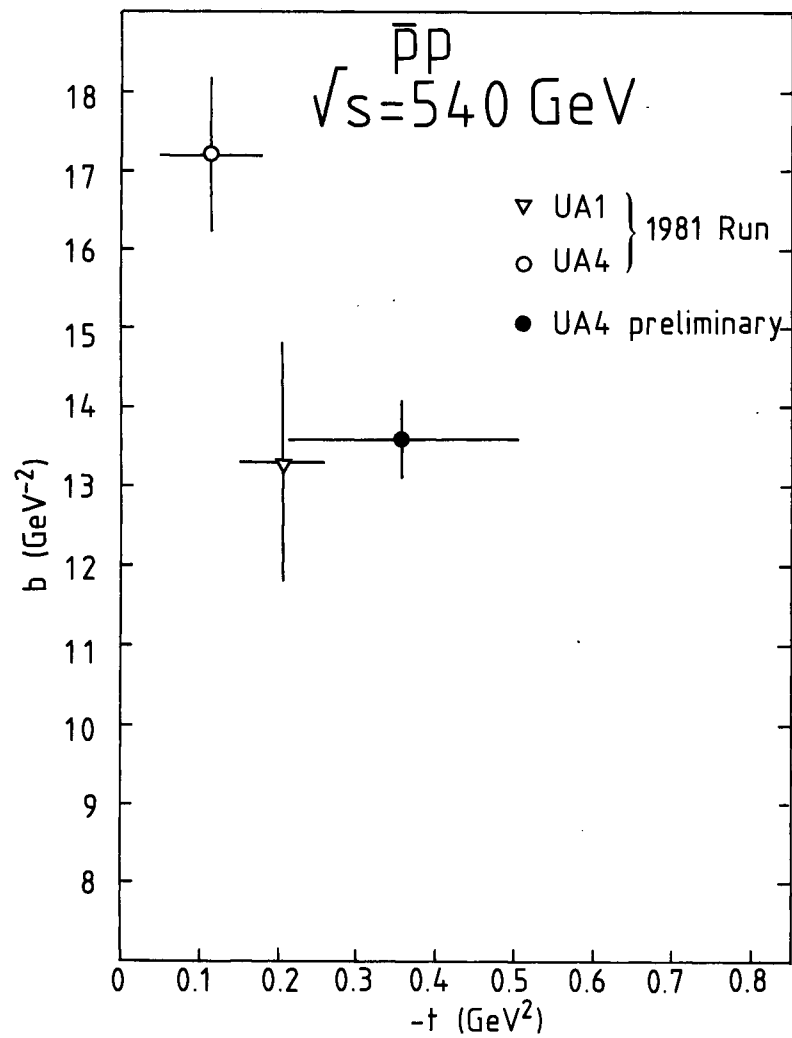


Fig. 5

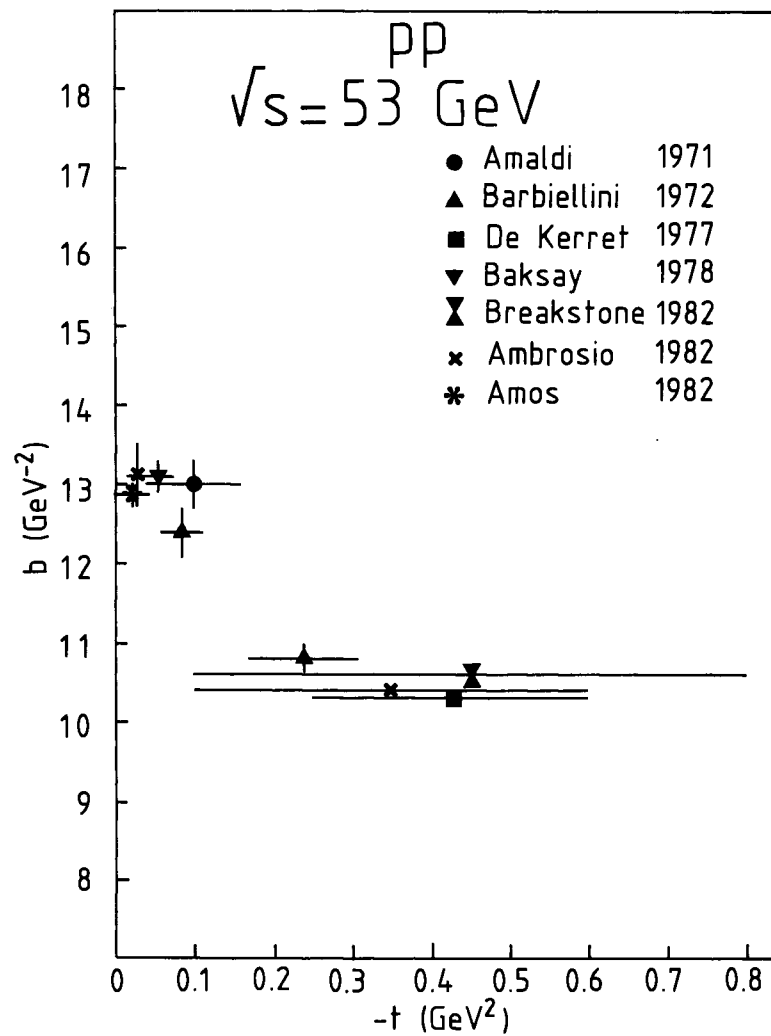


Fig. 6

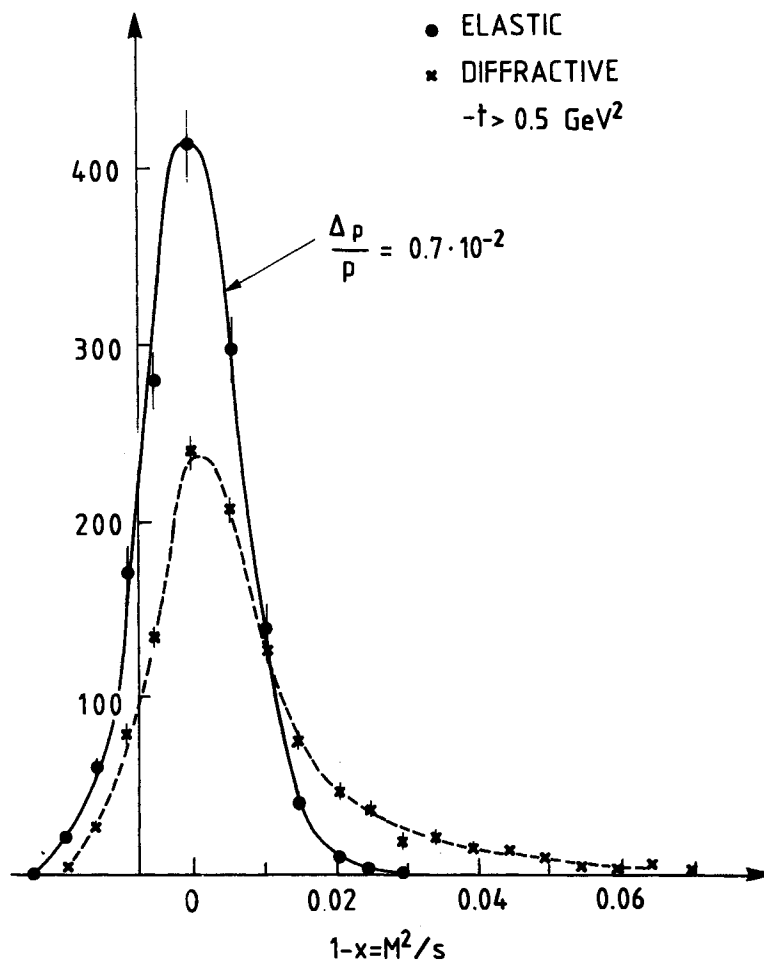


Fig. 7